

西藏拉萨地块过铝质花岗岩中继承锆石的物源区示踪及其古地理意义^{*}

朱弟成¹ 赵志丹¹ 牛耀龄^{2,3} 王青¹ DILEK Yildirim⁴ 管琪⁵ 刘勇胜⁶ 莫宣学¹

ZHU DiCheng¹, ZHAO ZhiDan¹, NIU YaoLing^{2,3}, WANG Qing¹, DILEK Yildirim⁴, GUAN Qi⁵, LIU YongSheng⁶ and MO XuanXue¹

1. 地质过程与矿产资源国家重点实验室,中国地质大学地球科学与资源学院,北京 100083

2. Department of Earth Sciences, Durham University, Durham DH1 3LE

3. 兰州大学地球科学学院,兰州 730000

4. Department of Geology, Miami University, Oxford, OH 45056

5. 石家庄经济学院资源学院,石家庄 050031

6. 地质过程与矿产资源国家重点实验室,中国地质大学地球科学学院,武汉 430074

1. State Key Laboratory of Geological Processes and Mineral Resources, and School of Earth Science and Mineral Resources, China University of Geosciences, Beijing 100083, China

2. Department of Earth Sciences, Durham University, Durham DH1 3LE, UK

3. School of Earth Sciences, Lanzhou University, Lanzhou 730000, China

4. Department of Geology, Miami University, Oxford, OH 45056, USA

5. College of Resources, Shijiazhuang University of Economics, Shijiazhuang 050031, China

6. State Key Laboratory of Geological Processes and Mineral Resources, and Faculty of Earth Sciences, China University of Geosciences, Wuhan 430074, China

2011-04-10 收稿, 2011-05-25 改回.

Zhu DC, Zhao ZD, Niu YL, Wang Q, Dilek Y, Guan Q, Liu YS and Mo XX. 2011. Tracing the provenance of inherited zircons from peraluminous granites in the Lhasa Terrane and its paleogeographic implications. *Acta Petrologica Sinica*, 27 (7):1917–1930

Abstract Peraluminous granites with abundant zircon inheritance are derived from partial melting of Al-rich rocks (e.g. metapelite). Thus the U-Pb age data of inherited zircons from peraluminous granites provide insights into provenance of clastic sediments in their source region, as do the detrital zircons from sedimentary rocks (and their metamorphosed equivalents). This paper reports the whole-rock geochemical and zircon U-Pb geochronological data (95 analyses) of the Early Jurassic peraluminous granites in the central Lhasa subterrane. These data, in combination with the existing data of inherited zircons (104 analyses) from the Permian and Late Triassic peraluminous granites currently available in the central Lhasa subterrane, are used to characterize the inherited zircon signature of the Lhasa Terrane. These granites belong to strongly peraluminous S-type granites, which contain abundant inherited zircons that define two main age populations of 1250 ~ 1100 Ma (peak at 1181 ± 14 Ma) and 550 ~ 450 Ma (peak at 494 ± 7 Ma), comparable to the ca. 1170 Ma age population defined by detrital zircons from Paleozoic sedimentary rocks and the emplacement timing of Cambrian volcanic rocks in the Lhasa Terrane, respectively. The ca. 1170 Ma age population defined by inherited and detrital zircons in the Lhasa Terrane differs significantly from the age distributions (peak at ca. 960 Ma) defined by detrital zircons from Neoproterozoic-Paleozoic sedimentary rocks in the western Qiangtang, Amdo, and Tethyan Hiamalaya in southern Tibet. We propose that the ca. 1181 Ma inherited zircons from peraluminous granites in the central Lhasa subterrane were most likely derived from the

* 本文受国家973项目(2011CB403102,2009CB421002)、国家自然科学面上基金项目(40973062,40973026)、中央高校基本科研业务费专项资金项目(2010ZD02)、教育部新世纪优秀人才项目(NCET-10-0711)、国家自然科学基金重点项目(40830317)和中国地质调查局工作项目(1212011121260,1212011121066)联合资助。

第一作者简介: 朱弟成,1972年生,男,博士,教授,主要从事岩浆作用与特提斯演化研究,E-mail: dchengzhu@163.com

Albany-Fraser orogenic belt in southwestern Australia and Wilkes Province in East Antarctica, as do the coeval detrital zircons from Paleozoic sedimentary rocks in the Lhasa Terrane, and that the ca. 494 Ma inherited zircons might have been sourced from both the Western Australia and Lhasa Terrane itself. This paper provides evidence of U-Pb dating on inherited zircons from peraluminous granites for the paleogeographic connection between the Lhasa Terrane and northern Australia. Our studies on the geology of the Lhasa Terrane indicate that a combined in-situ U-Pb dating on inherited zircons from peraluminous granites and detrital zircons from Paleozoic sedimentary rocks can provide important constraints on paleogeography and tectonomagmatic evolution of other microcontinents along the northern margin of Gondwana.

Key words Paleogeography; Lhasa-Australian connection; U-Pb ages of inherited zircons; Peraluminous granites; Lhasa Terrane

摘要 富含继承锆石的过铝质花岗岩一般来源于富铝质岩石(如变泥质岩)的部分熔融,因而分析这些继承锆石的U-Pb年龄可以像分析沉积岩碎屑锆石的U-Pb年龄一样,提供过铝质花岗岩源区物质中碎屑沉积物源区的丰富信息。本文报道了中部拉萨地块早侏罗世过铝质花岗岩的全岩地球化学和锆石U-Pb年代学数据,结合拉萨地块已有二叠纪和晚三叠世过铝质花岗岩的继承锆石年代学数据,总结了目前已有的拉萨地块过铝质花岗岩的继承锆石U-Pb年龄特征(共199个谐和测点)。这些过铝质花岗岩属强过铝质S型花岗岩,其中的继承锆石定义了1250~1100 Ma(峰值 1181 ± 14 Ma)和550~450 Ma(峰值 494 ± 7 Ma)2个最突出的年龄群,分别可比于拉萨地块古生代沉积岩的碎屑锆石年龄峰值(约1170 Ma)和寒武纪火山岩的侵位时代,明显不同于西羌塘、安多和特提斯喜马拉雅新元古代-古生代沉积岩中的碎屑锆石年龄频谱。拉萨地块过铝质花岗岩中约1181 Ma的继承锆石,可能与拉萨地块古生代沉积岩中的同期碎屑锆石一样,都来自澳大利亚南西部 Albany-Fraser造山带和东南极 Wilkes等地,而约494的继承锆石,既可能来自澳大利亚西部,也可能来自拉萨地块本地。本文提供了拉萨地块与澳大利亚大陆北缘具有古地理联系的过铝质花岗岩继承锆石U-Pb年龄证据。拉萨地块的研究实践表明,采用过铝质花岗岩继承锆石和古生代沉积岩碎屑锆石相结合的锆石U-Pb年代学方法,可为重建冈瓦纳大陆北缘其它微陆块的古地理和构造岩浆演化提供重要约束。

关键词 古地理; 拉萨-澳大利亚联系; 继承锆石U-Pb年龄; 过铝质花岗岩; 拉萨地块

中图法分类号 P588.121; P597.3

1 引言

基于和特提斯喜马拉雅相似的泛非期结晶基底和古生代-中生代沉积盖层、晚古生代冈瓦纳相动植物群和石炭-二叠纪冰海相沉积,拉萨地块长期以来被认为起源于印度大陆北缘(Sengör, 1987; Yin and Harrison, 2000; 潘桂棠等, 2004; Metcalfe, 2009; 李才等, 2009),但基于同样资料, Audley-Charles却赞成拉萨地块裂离自澳大利亚大陆北缘(Audley-Charles, 1983, 1984, 1988)。近年研究表明,拉萨地块二叠纪构造-岩浆作用所指示的大陆弧到同碰撞构造背景(潘桂棠等, 2006; Yang et al., 2009; 朱弟成等, 2009; Zhu et al., 2009a, 2010),明显不同于特提斯喜马拉雅和羌塘地区同期岩浆活动所指示的伸展背景。考虑到这种地球动力学体制的根本性差异,Zhu et al. (2009a, 2010)将拉萨地块从羌塘→拉萨→喜马拉雅这一连续的被动大陆边缘演化模型中抽取出来,置于古特提斯洋内,并认为其在中二叠世末期与澳大利亚大陆北缘发生了碰撞造山。这种推测的演化历史实际上暗示拉萨地块具有澳大利亚大陆亲缘性。最近在拉萨、羌塘和特提斯喜马拉雅奥陶纪-二叠纪变沉积岩中获得的大量碎屑锆石U-Pb年龄和Hf同位素数据,提供了拉萨地块与澳大利亚大陆具有古地理联系的直接证据(Zhu et al., 2011a)。

过铝质花岗岩在矿物学上以出现白云母、堇青石、石榴石、电气石和红柱石为特征,在地球化学上表现出高的铝饱和

和指数($A/CNK > 1.1$)和高的刚玉分子数(Miller, 1985; Sylvester, 1998)。由于过铝质花岗岩一般来源于富铝质岩石(如变泥质岩)的部分熔融,常富含继承锆石,因而与沉积岩碎屑锆石一样,可利用过铝质花岗岩中的继承锆石来示踪其源区物质中碎屑沉积物的物源区。本文目的是,报道拉萨地块当雄宁中、谷露地区早侏罗世过铝质花岗岩(图1)的全岩地球化学和锆石U-Pb年代学数据,在确认其岩石成因基础上,结合拉萨地块已有过铝质花岗岩(如罗扎、皮康花岗岩;图1)的继承锆石年代学数据,展示拉萨地块过铝质花岗岩的继承锆石年代学特征,讨论过铝质花岗岩源区物质中碎屑沉积物的物源区,为拉萨地块古地理重建提供进一步约束。

2 地质背景和样品

以龙木错-双湖缝合带(LSSZ)、班公湖-怒江缝合带(BNSZ)和印度河-雅鲁藏布缝合带(YYSZ)为界,从北向南可将西藏高原分为东羌塘(或北羌塘)、西羌塘(或南羌塘)、拉萨和喜马拉雅带4大地质构造单元,而进一步以狮泉河-纳木错蛇绿混杂岩带(SNMZ)和洛巴堆-米拉山断裂带(LMF)为界,由北向南可将其中的拉萨地块分为北部、中部和南部3部分(图1)(见:Zhu et al., 2012, 及其中参考文献)。

早期研究根据在安多地区发现的正片麻岩,认为北部拉萨地块存在寒武纪或新元古代结晶基底(Xu et al., 1985; Guynn et al., 2006)。但最近的研究表明,安多地区古生代

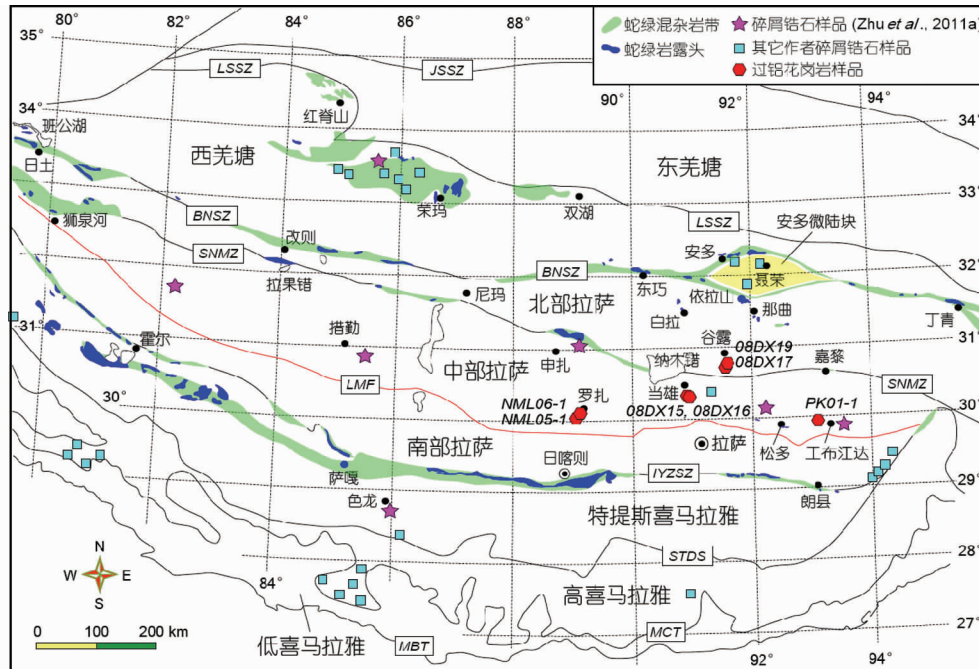


图1 西藏高原大地构造单元划分图及已有碎屑锆石和继承锆石样品分布位置(据 Zhu et al. , 2011a, 2012 修改)

新元古代-古生代变沉积岩碎屑锆石样品来源:西羌塘(Pullen et al. , 2008; Zhu et al. , 2011a; 董春艳等, 2011);安多(Guynn et al. , 2011);中部拉萨地块(Leier et al. , 2007; Zhu et al. , 2011a);南部拉萨地块(Dong et al. , 2010);特提斯喜马拉雅(McQuarrie et al. , 2008; Myrow et al. , 2010; Zhu et al. , 2011a);高喜马拉雅(Gehrels et al. , 2003, 2006a, 2006b)。过铝花岗岩样品来源:工布江达西皮康(Zhu et al. , 2009a);南木林罗扎(Zhu et al. , 2011b);当雄宁中和谷露地区(本文)

Fig. 1 Tectonic framework of the Tibetan Plateau showing the localities of detrital zircon and inherited zircon samples (modified after Zhu et al. , 2011a, 2012)

副变质岩具有完全不同于中部拉萨地块古生代沉积岩的碎屑锆石年龄频谱,这意味着不能再把安多微陆块作为拉萨地块的一部分来考虑(Zhu et al. , 2012)。现今意义上位于安多微陆块南部的北部拉萨地块,以新生地壳为特征,上覆中三叠统到白垩系沉积盖层,富含丰富的早白垩世火山岩和同期花岗岩类(朱弟成等, 2006; Zhu et al. , 2011b, 2012)。中部拉萨地块是一个具有元古代和太古代结晶基底的微陆块(Zhu et al. , 2009a, 2011b, 2012)。这些基底岩石(如部分念青唐古拉群变质岩)经历了新元古代(约 720Ma; 张泽明等, 2010)、晚三叠世(225 ~ 213Ma; Dong et al. , 2011)和新生代(Xu et al. , 1985; Kapp et al. , 2005)多期变质作用。这种变质基底上覆广泛出露的石炭-二叠系和上侏罗统-下白垩统沉积岩以及大量早白垩世火山岩和中生代花岗岩类(莫宣学等, 2005; 朱弟成等, 2006, 2008; 张宏飞等, 2007; Zhu et al. , 2009a, 2011b, 2012),另外还有少量保存极好的奥陶系、志留系、泥盆系和三叠系灰岩(Pan et al. , 2004)以及少量寒武纪变火山沉积岩(计文化等, 2009)。南部拉萨地块以新生地壳为特征(莫宣学等, 2005; Mo et al. , 2007, 2008; Ji et al. , 2009; Zhu et al. , 2011b),目前并未发现寒武纪结晶基底(Dong et al. , 2010; Zhu et al. , 2012)。该地块以白垩纪-第三纪冈底斯岩基(莫宣学等, 2005; Ji et al. , 2009)

和古近纪林子宗火山岩为主(Mo et al. , 2007, 2008; Lee et al. , 2009; Zhu et al. , 2011b),在其东部有少量三叠纪最晚期-白垩纪火山沉积岩出露(Pan et al. , 2004; Zhu et al. , 2008, 2012)。

一般认为,拉萨地块不但一个与印度-欧亚大陆碰撞有关的新生代造山带,还是一个与新特提斯大洋岩石圈北向俯冲有关的前新生代安第斯型活动大陆边缘(Allègre et al. , 1984; Sengör, 1987; Yin and Harrison, 2000; Chung et al. , 2005; Zhang et al. , 2010; Zhu et al. , 2011b)。最近的研究表明,新特提斯大洋岩石圈的北向俯冲可能开始于早白垩世早期,由羌塘-拉萨碰撞所激发,拉萨地块上的大多数中生代岩浆作用很可能与班公湖-怒江大洋岩石圈的南向俯冲有关,这一俯冲开始于中二叠世末期的拉萨-澳大利亚碰撞,结束于早白垩世晚期(Zhu et al. , 2009a, b, 2010, 2011b, 2012)。

本文报道的过铝质花岗岩位于中部拉萨地块东部当雄宁中及其北侧谷露等地(图1)。刘琦胜等(2006)报道了宁中地区的早侏罗世过铝质花岗岩(约 193Ma)。这些花岗岩呈岩瘤状侵位于石炭-二叠系变沉积岩中,岩石类型包括灰白色中粗粒二云母花岗岩、灰白色粗粒黑云母花岗岩和灰白色粗粒二长花岗岩等。

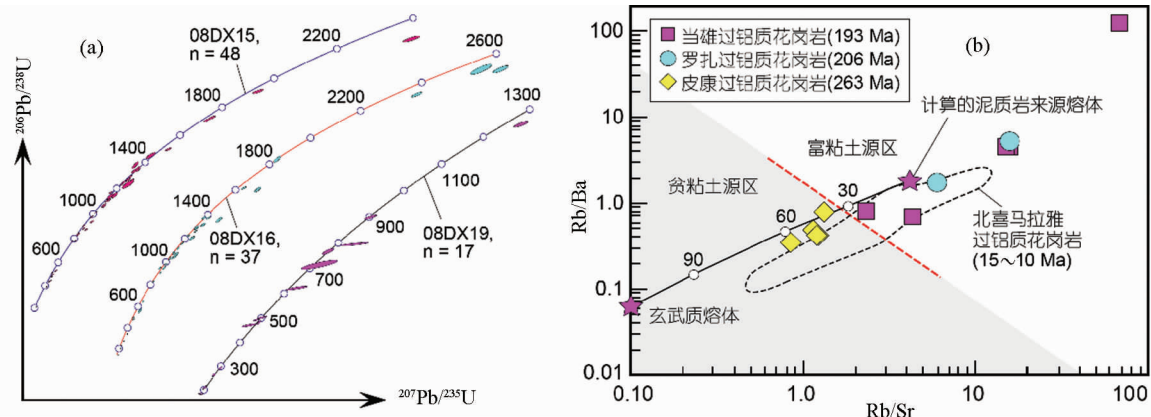


图 2 拉萨地块早侏罗世过铝质花岗岩锆石 U-Pb 年龄谐和图(a)和全岩 Rb/Ba-Rb/Sr 图(据 Sylvester, 1998)

北喜马拉雅过铝质花岗岩(15~10Ma; Zhang et al., 2004);罗扎过铝质花岗岩(约206Ma; Zhu et al., 2011a);皮康过铝质花岗岩(约263Ma; Zhu et al., 2009a)

Fig. 2 Concordia plot for single zircon analyzed by LA-ICPMS U-Pb (a) and Rb/Ba vs. Rb/Sr plot (b, after Sylvester, 1998) for the Early Jurassic peraluminous granites in the Lhasa Terrane

3 分析方法

样品主量元素和微量元素分析在中国地质大学(武汉)地质过程与矿产资源国家重点实验室(GPMR)进行。主量元素由XRF法测试,微量元素由ICP-MS法测试。测试过程中,根据同时测定的BHVO-1、AGV-1和G-2等标样来监测测试精度,具体的测试方法详见(Liu et al., 2008)。锆石是在河北廊坊物化勘查研究所采用浮选和电磁选方法完成的。锆石阴极发光图像在中国地质科学院完成。利用锆石阴极发光图像,重点选择锆石的继承核部进行U-Pb同位素定年。锆石U-Pb定年在中国地质大学(武汉)地质过程与矿产资源国家重点实验室利用LA-ICP-MS分析完成。测试仪器为Agilent 7500a,激光剥蚀系统为GeoLas 2005。每个时间分辨分析数据包括大约20~30s的空白信号和50s的样品信号。采用软件ICPMSDataCal软件(Liu et al., 2008, 2010)对分析数据进行离线处理(包括对样品和空白信号的选择、仪器灵敏度漂移校正、元素含量及U-Th-Pb同位素比值和年龄计算),采用Andersen(2002)方法(ComPbCorr[#]3-151程序)进行普通铅校正。详细的仪器操作条件和数据处理方法见Liu et al. (2008, 2010)。本文不考虑谐和度大于10%的测点,同时对大于1000Ma的锆石,采用 $^{207}\text{Pb}/^{206}\text{Pb}$ 年龄,对小于1000Ma的锆石,采用 $^{206}\text{Pb}/^{238}\text{U}$ 年龄。

4 分析结果

4.1 锆石 U-Pb 年代学

本文对当雄宁中(样品08DX15, 08DX16)和谷露(样品08DX19)两地的3件过铝质花岗岩样品进行了锆石U-Pb定

年(图2a和表1)。这些过铝质花岗岩中的锆石显示2种形态:一种呈浑圆状,核部为灰白色,大多数均有宽的黑色生长边;另一种为长柱状(长宽比为2:1~4:1),黑色生长边较薄或无。样品08DX16中,具有完好岩浆锆石的自形柱状晶型的一颗锆石给出的 $^{206}\text{Pb}/^{238}\text{U}$ 年龄为 $195 \pm 2\text{ Ma}$ (Th/U=0.87),与宁中地区报道的过铝质花岗岩浆活动(约193Ma;刘琦胜等,2006)同期。黑色生长边具有高的U含量, Th/U比值均小于0.1,对应的 $^{206}\text{Pb}/^{238}\text{U}$ 年龄分别为175~173Ma(样品08DX15)、 $190 \pm 1\text{ Ma}$ (样品08DX16)和184~181Ma(样品08DX19)(表1),与胡道功等(2004)在纳木错西岸斜长角闪质麻粒岩中获得的角闪石 $^{40}\text{Ar}/^{39}\text{Ar}$ 年龄(约174Ma)基本同期,表明当雄地区这些早侏罗世岩浆岩经历了稍晚期变质事件的改造。锆石核部给出了较为宽泛的U-Pb年龄值,介于202~2705Ma之间(表1),其中202Ma的继承锆石年齡值,与Kapp et al. (2005)在当雄地区二云母花岗岩中获得的继承锆石年齡(204Ma)相当。

4.2 全岩地球化学

当雄宁中、谷露地区过铝质花岗岩的SiO₂含量变化于69.85%~75.34%,K₂O含量(3.87%~5.99%)较高,Na₂O含量(2.40%~4.01%)较低,具有高的铝饱和指数(A/CNK=1.14~1.31)和刚玉分子数(1.75%~4.18%)(表2)。在谷露地区一件同期过铝质花岗岩样品(08DX17)的锆石 $\varepsilon_{\text{HF}}(t)$ 值为大的负值(变化于-20.5~-16.0; Zhu et al., 2011b),结合岩石中出现的富Al矿物(如白云母)和高的Rb/Sr比值(2.3~68.5)(图2b),表明这些岩石与罗扎强过铝质花岗岩一样(张宏飞等,2007),均属成熟地壳物质(如变泥质岩)部分熔融产生的强过铝质S型花岗岩。皮康过铝质花岗岩略有不同,其相对较低Rb/Sr比值,可能与来源于成熟地壳的过铝质花岗岩熔体中混入了较多幔源物质(约30%;

表 1 拉萨地块早侏罗世过铝质花岗岩继承锆石 U-Pb 年龄数据

Table 1 U-Pb age data of inherited zircons from the Early Jurassic peraluminous granites in the Lhasa Terrane

测点号	元素丰度 ($\times 10^{-6}$)			普通铅校正后的同位素比值						普通铅校正后的同位素年龄 (Ma)						不谐和度 (%)	接受年龄 ($\pm 1\sigma$; Ma)	
	Pb	Th	U	* Pb ²⁰⁷ /* Pb ²⁰⁶	* Pb ²⁰⁷ /* U ²³⁵	* Pb ²⁰⁶ /* U ²³⁸	($\pm 1\sigma$)	* Pb ²⁰⁷ /* Pb ²⁰⁶	* Pb ²⁰⁷ /* U ²³⁵	* Pb ²⁰⁶ /* U ²³⁸	($\pm 1\sigma$)							
样品 08DX15 的最年轻谱和年龄: 第 56、60 测点, 年龄分别 175 ± 1 Ma 和 173 ± 1 Ma																		
08DX15_01	24	169	254	0.67	0.0554	0.0011	0.6222	0.0119	0.0812	0.0006	429	29	491	7	503	4	2.4	503
08DX15_02	115	337	681	0.50	0.0682	0.0008	1.4188	0.0196	0.1500	0.0011	875	17	897	8	901	6	0.4	901
08DX15_03	61	265	195	1.36	0.0844	0.0014	2.6709	0.0432	0.2293	0.0022	1302	17	1320	12	1331	11	0.8	1302
08DX15_04	13	113	127	0.89	0.0613	0.0020	0.7120	0.0216	0.0844	0.0009	651	47	546	13	522	5	-4.6	522
08DX15_05	39	188	258	0.73	0.0633	0.0011	1.1118	0.0189	0.1269	0.0008	718	25	759	9	770	5	1.4	770
08DX15_06	46	143	147	0.97	0.0891	0.0021	3.0978	0.0710	0.2519	0.0029	1406	26	1432	18	1448	15	1.1	1406
08DX15_08	139	174	576	0.30	0.0855	0.0010	2.7505	0.0428	0.2321	0.0024	1327	16	1342	12	1345	12	0.2	1327
08DX15_09	27	205	140	1.46	0.0668	0.0017	1.2727	0.0301	0.1382	0.0012	830	35	834	13	834	7	0.0	834
08DX15_10	98	215	625	0.34	0.0700	0.0009	1.4113	0.0196	0.1455	0.0011	929	16	894	8	876	6	-2.1	876
08DX15_11	45	96	209	0.46	0.0760	0.0011	2.0794	0.0295	0.1976	0.0013	1096	18	1142	10	1163	7	1.8	1096
08DX15_12	39	137	208	0.66	0.0719	0.0011	1.6193	0.0259	0.1627	0.0011	982	21	978	10	972	6	-0.6	972
08DX15_13	97	247	206	1.20	0.1210	0.0018	5.7758	0.0854	0.3445	0.0022	1971	17	1943	13	1908	10	-1.8	1971
08DX15_14	141	201	554	0.36	0.0864	0.0010	2.7624	0.0353	0.2310	0.0016	1347	14	1345	10	1340	9	-0.4	1347
08DX15_16	73	240	340	0.71	0.0780	0.0010	1.9185	0.0249	0.1778	0.0009	1148	18	1088	9	1055	5	-3.1	1148
08DX15_18	43	137	274	0.50	0.0665	0.0013	1.2566	0.0248	0.1370	0.0012	821	27	826	11	827	7	0.1	827
08DX15_19	117	308	531	0.58	0.0788	0.0012	2.0346	0.0311	0.1868	0.0014	1168	19	1127	10	1104	7	-2.1	1168
08DX15_20	12	110	346	0.32	0.0503	0.0015	0.2206	0.0063	0.0321	0.0003	209	50	202	5	204	2	1.0	204
08DX15_24	153	329	479	0.69	0.0982	0.0013	3.5353	0.0474	0.2605	0.0015	1591	17	1535	11	1492	7	-2.9	1591
08DX15_26	51	173	344	0.50	0.0676	0.0012	1.1922	0.0213	0.1279	0.0009	856	26	797	10	776	5	-2.7	776
08DX15_27	167	165	836	0.20	0.0777	0.0012	1.9896	0.0274	0.1858	0.0010	1138	30	1112	9	1099	6	-1.2	1138
08DX15_29	51	149	306	0.49	0.0737	0.0012	1.4700	0.0237	0.1445	0.0012	1033	20	918	10	870	7	-5.5	870
08DX15_30	33	94	152	0.62	0.0778	0.0013	1.9154	0.0335	0.1790	0.0019	1141	19	1086	12	1061	10	-2.4	1141
08DX15_31	32	183	457	0.40	0.0574	0.0012	0.4882	0.0116	0.0614	0.0007	508	33	404	8	384	4	-5.2	384
08DX15_32	60	144	149	0.97	0.1091	0.0015	4.6239	0.0654	0.3066	0.0017	1784	18	1754	12	1724	8	-1.7	1784
08DX15_33	50	289	616	0.47	0.0606	0.0010	0.5888	0.0103	0.0703	0.0004	623	27	470	7	438	3	-7.3	438
08DX15_34	51	557	1461	0.38	0.0504	0.0008	0.2221	0.0033	0.0319	0.0002	215	26	204	3	202	1	-0.8	202
08DX15_35	29	309	293	1.05	0.0584	0.0013	0.6136	0.0140	0.0761	0.0006	546	37	486	9	473	3	-2.7	473
08DX15_36	168	34	776	0.04	0.0873	0.0011	2.6126	0.0323	0.2165	0.0012	1367	16	1304	9	1263	6	-3.2	1367
08DX15_37	11	107	326	0.33	0.0505	0.0017	0.2220	0.0079	0.0319	0.0003	216	65	204	7	202	2	-1.0	202
08DX15_38	26	287	272	1.05	0.0572	0.0013	0.5987	0.0136	0.0759	0.0007	500	35	476	9	471	4	-1.1	471
08DX15_39	22	198	230	0.86	0.0582	0.0013	0.6355	0.0140	0.0792	0.0005	537	37	500	9	491	3	-1.8	491
08DX15_40	112	749	389	1.92	0.0778	0.0009	2.0298	0.0242	0.1888	0.0010	1141	15	1126	8	1115	6	-1.0	1141
08DX15_42	89	513	242	2.12	0.0821	0.0013	2.6960	0.0493	0.2378	0.0030	1248	18	1327	14	1375	16	3.5	1248

续表 1
Continued Table 1

测点号	元素丰度 ($\times 10^{-6}$)			普通铅校正后的同位素比值						普通铅校正后的同位素年龄 (Ma)						
	Pb	Th	U	$^{207}\text{Pb}/^{206}\text{Pb}$			$* \text{Pb}_{207}^{207}/\text{U}^{235}$			$* \text{Pb}_{206}^{206}/\text{U}^{238}$			$\text{Pb}_{207}^{207}/\text{Pb}_{206}^{206}$			
				($\pm 1\sigma$)			($\pm 1\sigma$)			($\pm 1\sigma$)			($\pm 1\sigma$)			
08DX15 43	41	100	168	0.60	0.0868	0.0037	2.5163	0.0955	0.2102	0.0042	1357	85	1277	28	1230	22
08DX15 44	115	838	1410	0.59	0.0571	0.0008	0.5444	0.0079	0.0690	0.0006	495	17	441	5	430	4
08DX15 46	218	341	958	0.36	0.0814	0.0009	2.3640	0.0269	0.0014	0.0020	1231	13	1232	8	1228	7
08DX15 47	74	130	307	0.42	0.0837	0.0013	2.5014	0.0414	0.2161	0.0020	1284	18	1272	12	1261	11
08DX15 48	25	116	99	1.17	0.0780	0.0017	2.0787	0.0498	0.1927	0.0024	1147	28	1142	16	1136	13
08DX15 50	48	134	185	0.72	0.0820	0.0011	2.4251	0.0358	0.2137	0.0015	1245	18	1250	11	1249	8
08DX15 51	134	745	392	1.90	0.0840	0.0010	2.5692	0.0303	0.2212	0.0012	1293	14	1292	9	1288	7
08DX15 52	82	31	522	0.06	0.0752	0.0017	1.6153	0.0343	0.1558	0.0013	1073	47	976	13	933	7
08DX15 53	82	619	896	0.69	0.0570	0.0010	0.6045	0.0109	0.0768	0.0006	490	26	480	7	477	4
08DX15 55	120	86	582	0.15	0.0815	0.0021	2.1798	0.0482	0.1940	0.0026	1234	52	1175	15	1143	14
08DX15 56	439	1238	15819	0.08	0.0546	0.0009	0.2077	0.0030	0.0276	0.0002	396	39	192	3	175	1
08DX15 57	99	52	563	0.09	0.0736	0.0010	1.7200	0.0222	0.1696	0.0009	1030	29	1016	8	1010	5
08DX15 58	36	57	64	0.90	0.1653	0.0022	9.6151	0.1386	0.4209	0.0029	2511	15	2399	13	2264	13
08DX15 59	165	216	466	0.46	0.1071	0.0012	4.4842	0.0516	0.3027	0.0017	1751	13	1728	10	1705	8
08DX15 60	390	608	14466	0.04	0.0496	0.0007	0.1863	0.0022	0.0273	0.0001	174	31	173	2	173	1
样品 08DX16 的最年轻和年龄: 第 18、34 测点, 年龄分别 195 ± 2 Ma 和 190 ± 1 Ma																
08DX16 01	99	183	286	0.64	0.1040	0.0013	4.0811	0.0517	0.2838	0.0015	1696	16	1651	10	1611	7
08DX16 02	35	89	125	0.72	0.0897	0.0016	2.7910	0.0469	0.2259	0.0018	1418	20	1353	13	1313	9
08DX16 03	100	171	169	1.01	0.1587	0.0019	9.4734	0.1129	0.4319	0.0027	2442	12	2285	11	2314	12
08DX16 05	45	48	1086	0.04	0.0561	0.0010	0.3280	0.0075	0.0420	0.0005	456	30	288	6	265	3
08DX16 06	67	208	365	0.57	0.0667	0.0011	1.4535	0.0255	0.1575	0.0010	830	26	911	11	943	5
08DX16 07	191	472	1039	0.45	0.0721	0.0012	1.6286	0.0264	0.1633	0.0009	989	24	981	10	975	5
08DX16 08	11	100	109	0.92	0.0562	0.0016	0.6104	0.0165	0.0792	0.0007	459	44	484	10	492	4
08DX16 09	201	316	879	0.36	0.0808	0.0010	2.3356	0.0299	0.2089	0.0013	1217	15	1223	9	1223	7
08DX16 10	18	27	521	0.05	0.0506	0.0011	0.2445	0.0053	0.0352	0.0003	220	32	222	4	223	2
08DX16 11	49	194	310	0.63	0.0667	0.0012	1.2558	0.0220	0.1363	0.0011	827	23	826	10	824	6
08DX16 12	100	284	450	0.63	0.0776	0.0011	2.0273	0.0291	0.1887	0.0012	1137	18	1125	10	1115	7
08DX16 13	109	125	299	0.42	0.1123	0.0015	5.1153	0.0801	0.3293	0.0034	1836	14	1839	13	1835	17
08DX16 14	221	325	804	0.40	0.1026	0.0023	3.3109	0.0627	0.2340	0.0026	1672	42	1484	15	1355	14
08DX16 15	90	177	486	0.36	0.0739	0.0010	1.7567	0.0273	0.1721	0.0018	1039	16	1030	10	1023	10
08DX16 16	47	87	176	0.49	0.0858	0.0011	2.8173	0.0405	0.2371	0.0017	1335	17	1360	11	1372	9
08DX16 17	147	101	809	0.12	0.0757	0.0013	1.8908	0.0282	0.1813	0.0016	1086	36	1078	10	1074	9
08DX16 18	70	1647	1883	0.87	0.0496	0.0009	0.2112	0.0045	0.0307	0.0003	178	29	195	4	195	2
08DX16 19	26	59	37	1.57	0.1765	0.0031	11.5031	0.2245	0.4717	0.0054	2620	18	2565	18	2491	23

接受年齡
($\pm 1\sigma; \text{Ma}$)不谐和
度 (%)($\pm 1\sigma$)

Continued Table 1

测点号	元素丰度 ($\times 10^{-6}$)			普通铅校正后的同位素比值						普通铅校正后的同位素年龄 (Ma)						不谐和度 (%) ($\pm 1\sigma$)	接受年龄 ($\pm 1\sigma$; Ma)		
	Pb	Th	U	$^{207}\text{Pb}/^{206}\text{Pb}$			$^{207}\text{Pb}/^{235}\text{U}$			$^{206}\text{Pb}/^{238}\text{U}$			$^{207}\text{Pb}/^{206}\text{Pb}$						
				($\pm 1\sigma$)			($\pm 1\sigma$)			($\pm 1\sigma$)			($\pm 1\sigma$)						
08DX16 20	125	318	598	0.53	0.0794	0.0015	1.9385	0.0337	0.1770	0.0010	1183	37	1094	12	1050	5	-4.2	1183	37
08DX16 21	33	184	577	0.32	0.0579	0.0013	0.4267	0.0111	0.0532	0.0007	526	35	361	8	334	4	-8.1	334	4
08DX16 23	394	783	1435	0.55	0.0902	0.0012	2.9608	0.0389	0.2369	0.0012	1430	17	1398	10	1371	6	-2.0	1430	17
08DX16 24	88	195	445	0.44	0.0782	0.0019	1.8768	0.0430	0.1740	0.0013	1153	49	1073	15	1034	7	-3.8	1153	49
08DX16 25	28	169	103	1.64	0.0795	0.0018	1.9592	0.0464	0.1786	0.0022	1184	27	1102	16	1059	12	-4.1	1184	27
08DX16 26	209	113	693	0.16	0.1154	0.0015	4.4958	0.0669	0.2813	0.0027	1886	14	1730	12	1598	13	-8.3	1886	14
08DX16 27	73	245	416	0.59	0.0706	0.0010	1.4644	0.0208	0.1499	0.0011	946	17	916	9	900	6	-1.8	900	6
08DX16 28	31	56	125	0.45	0.0844	0.0013	2.5906	0.0421	0.2221	0.0019	1301	18	1298	12	1293	10	-0.4	1301	18
08DX16 29	119	258	521	0.50	0.0786	0.0012	2.1415	0.0305	0.1969	0.0015	1163	16	1162	10	1158	8	-0.3	1163	16
08DX16 30	22	139	168	0.83	0.0638	0.0015	0.9227	0.0237	0.1046	0.0013	733	33	664	12	641	8	-3.6	641	8
08DX16 33	43	163	986	0.16	0.0529	0.0015	0.3008	0.0082	0.0413	0.0003	323	66	267	6	261	2	-2.3	261	2
08DX16 34	377	359	12172	0.03	0.0515	0.0010	0.2122	0.0037	0.0299	0.0002	265	45	195	3	190	1	-2.6	190	1
08DX16 35	103	162	414	0.39	0.0848	0.0015	2.5732	0.0415	0.2202	0.0013	1310	34	1293	12	1283	7	-0.8	1310	34
08DX16 36	133	206	1412	0.15	0.0661	0.0032	0.8131	0.0344	0.0893	0.0021	808	104	604	19	551	13	-9.6	551	13
08DX16 37	19	115	219	0.52	0.0583	0.0015	0.6143	0.0165	0.0764	0.0008	542	41	486	10	475	5	-2.3	475	5
08DX16 38	53	141	299	0.47	0.0733	0.0012	1.5941	0.0305	0.1575	0.0015	1021	24	968	12	943	8	-2.7	943	8
08DX16 40	174	261	268	0.97	0.1857	0.0021	12.1095	0.1609	0.4720	0.0039	2705	12	2613	12	2492	17	-4.9	2705	12
08DX16 41	180	189	777	0.24	0.0861	0.0009	2.5683	0.0282	0.2161	0.0012	1340	13	1292	8	1261	6	-2.5	1340	13
08DX16 42	57	94	246	0.38	0.0866	0.0017	2.4511	0.0545	0.2047	0.0020	1351	28	1258	16	1201	11	-4.7	1351	28
样品08DX19 的最年轻谐和年龄: 第02,09 测点, 年龄分别为 184 ± 2 Ma 和 181 ± 1 Ma																			
08DX19 01	80	555	849	0.65	0.0556	0.0015	0.6071	0.0166	0.0791	0.0005	436	51	482	10	491	3	1.8	491	3
08DX19 02	29	68	1007	0.07	0.0486	0.0017	0.1939	0.0071	0.0289	0.0003	126	69	180	6	184	2	2.2	184	2
08DX19 04	307	1446	2064	0.70	0.0659	0.0055	1.0627	0.0867	0.1169	0.0021	803	181	735	43	713	12	-3.1	713	12
08DX19 05	91	393	787	0.50	0.0645	0.0034	0.8994	0.0508	0.1010	0.0008	758	107	651	27	620	5	-5.0	620	5
08DX19 07	36	282	411	0.69	0.0531	0.0032	0.5533	0.0350	0.0756	0.0008	334	125	447	23	470	5	4.9	470	5
08DX19 08	91	469	614	0.76	0.0730	0.0035	1.3181	0.0666	0.1311	0.0008	1013	94	854	29	794	4	-7.6	794	4
08DX19 09	28	71	997	0.07	0.0519	0.0026	0.2036	0.0102	0.0285	0.0002	281	101	188	9	181	1	-3.9	181	1
08DX19 10	53	266	587	0.45	0.0580	0.0020	0.6460	0.0228	0.0808	0.0006	530	65	506	14	501	4	-1.0	501	4
08DX19 11	59	79	1470	0.05	0.0516	0.0018	0.2960	0.0093	0.0416	0.0007	269	83	263	7	263	4	0.0	263	4
08DX19 12	34	185	174	1.06	0.0697	0.0013	1.4372	0.0284	0.1496	0.0010	918	30	905	12	899	5	-0.7	899	5
08DX19 13	156	447	1112	0.40	0.0649	0.0017	1.1275	0.0271	0.1260	0.0014	771	57	767	13	765	8	-0.3	765	8
08DX19 14	159	75	716	0.10	0.0863	0.0013	2.5323	0.0345	0.2129	0.0014	1344	30	1281	10	1244	7	-3.0	1344	30
08DX19 18	61	67	1882	0.04	0.0514	0.0008	0.2412	0.0040	0.0340	0.0003	260	23	219	3	216	2	-1.4	216	2
08DX19 19	67	146	1531	0.10	0.0537	0.0009	0.3430	0.0089	0.0461	0.0008	359	29	299	7	290	5	-3.1	290	5
08DX19 20	192	3048	1744	1.75	0.0581	0.0008	0.6209	0.0107	0.0774	0.0009	533	19	490	7	481	5	-1.9	481	5
08DX19 22	120	639	3251	0.20	0.0500	0.0023	0.2277	0.0090	0.0330	0.0008	195	109	208	7	209	5	0.5	209	5

注: * 指放射性成因铅; 同位素比值和年龄使用 Andersen (2002) 方法校正

表 2 拉萨地块晚三叠世-早侏罗世过铝质花岗岩全岩地球化学数据(主量元素:wt%;稀土和微量元素: $\times 10^{-6}$)Table 2 Whole-rock geochemical data of the Late Triassic-Early Jurassic peraluminous granites in the Lhasa Terrane (Major elements: wt%; Trace elements: $\times 10^{-6}$)

样品号	08DX15	08DX16	08DX17 [*]	08DX18	08DX19	NML05-1 [*]	NML06-1 [*]
岩石名称	灰白色中粗粒 二云母花岗岩	灰白色粗粒 黑云母花岗岩	灰白色粗粒 二长花岗岩	灰白色粗粒 二长花岗岩	灰白色粗粒 二云母花岗岩	灰白色中细粒 二云母花岗岩	灰白色中细粒 二云母花岗岩
年龄(Ma)	193	193	193	193	193	206	206.5
SiO ₂	72.15	75.34	69.85	74.51	75	73.17	74.58
TiO ₂	0.08	0.07	0.27	0.16	0.03	0.21	0.07
Al ₂ O ₃	15.67	14.35	15.34	13.08	14.74	14.37	14.62
Fe ₂ O ₃ ^T	1.27	0.47	2.52	2.38	0.73	1.68	1.17
MnO	0.04	0.02	0.03	0.04	0.04	0.02	0.03
MgO	0.17	0.21	0.80	0.24	0.09	0.41	0.19
CaO	0.37	0.48	1.22	0.35	0.54	0.70	0.65
Na ₂ O	3.09	2.59	2.40	2.89	4.01	2.68	3.69
K ₂ O	5.91	5.36	5.99	5.63	3.87	5.52	4.33
P ₂ O ₅	0.26	0.24	0.31	0.06	0.35	0.19	0.20
烧失量	1.22	1.24	1.08	1.01	1.01	0.70	0.64
总量	100.23	100.37	99.81	100.35	100.41	99.65	100.17
A/CNK	1.29	1.31	1.21	1.14	1.25	1.23	1.23
CIPW 标准矿物							
石英(Q)	31.3	39.4	30.0	35.0	36.6	35.0	35.3
钙长石(An)	0.14	0.82	4.09	1.36	0.4	2.26	1.93
钠长石(Ab)	26.4	22.1	20.6	24.7	34.2	22.9	31.4
正长石(Or)	35.3	32.0	35.9	33.5	23.0	33	25.7
刚玉(C)	4.18	4.03	3.48	1.75	3.83	3.2	3.18
紫苏辉石(Hy)	1.05	0.73	3.11	1.74	0.69	1.71	1.11
钛铁矿(II)	0.15	0.13	0.52	0.31	0.06	0.4	0.13
磁铁矿(Mt)	0.84	0.30	1.60	1.54	0.45	1.07	0.73
磷灰石(Ap)	0.61	0.56	0.73	0.14	0.82	0.45	0.47
Sc	4.62	3.78	3.69	6.07	2.04	2.48	1.77
V	4.71	4.39	23.0	8.32	1.11	8.77	1.49
Cr	3.03	3.05	13.0	2.11	1.72	6.34	2.20
Co	1.34	0.62	4.28	1.66	0.19	1.76	0.65
Ni	1.20	0.72	6.38	1.03	0.35	1.95	0.58
Ga	19.6	18.2	18.4	18.1	25.4	22.5	19.6
Rb	577	523	304	273	757	387	427
Sr	36	35	131	63	11	64	27
Y	9.61	9.25	13.2	37.0	11.0	12.8	9.45
Zr	39.3	42.6	148.9	228.1	42.6	119.5	38.5
Nb	28.1	20.5	18.4	15.1	48.1	14.5	18.6
Cs	74.6	62.6	15.8	12.5	103.2	9.4	18.1
Ba	131	119	381	392	6.0	233	84
La	9.44	7.34	45.23	109.8	9.63	46.19	8.14
Ce	20.8	16.2	95.1	205.1	20.9	102.6	16.5
Pr	2.35	1.88	11.60	22.3	2.51	11.7	1.82
Nd	8.59	7.09	43.40	77.1	9.21	46.1	7.04
Sm	2.38	2.07	8.77	12.0	2.40	8.92	1.77
Eu	0.42	0.41	1.13	0.96	0.11	0.58	0.28
Gd	2.41	2.27	6.23	9.13	2.36	5.32	1.66
Tb	0.43	0.42	0.76	1.31	0.39	0.59	0.31
Dy	2.07	2.11	3.08	7.15	2.06	2.62	1.69
Ho	0.31	0.32	0.49	1.42	0.35	0.43	0.28
Er	0.72	0.72	1.08	3.70	0.91	1.09	0.66
Tm	0.11	0.10	0.15	0.54	0.13	0.14	0.09
Yb	0.63	0.61	0.89	3.57	0.77	0.94	0.56
Lu	0.09	0.08	0.13	0.54	0.10	0.13	0.07
Hf	1.47	1.51	4.32	6.48	1.81	3.41	1.41
Ta	6.87	4.81	1.78	1.47	10.90	2.08	4.89
Pb	52.3	43.7	66.5	29.3	19.9	75.1	33.4
Th	6.22	6.66	33.1	35.3	7.05	48.9	6.84
U	18.7	3.12	5.51	3.12	3.33	4.38	2.28
Rb/Sr	15.9	15.1	2.3	4.3	68.5	6.0	15.9
Rb/Ba	4.4	4.4	0.8	0.7	123.7	1.7	5.1

注: * 引用自 Zhu et al. (2011b). A/CNK = 摩尔数 $Al_2O_3/(CaO + Na_2O + K_2O)$

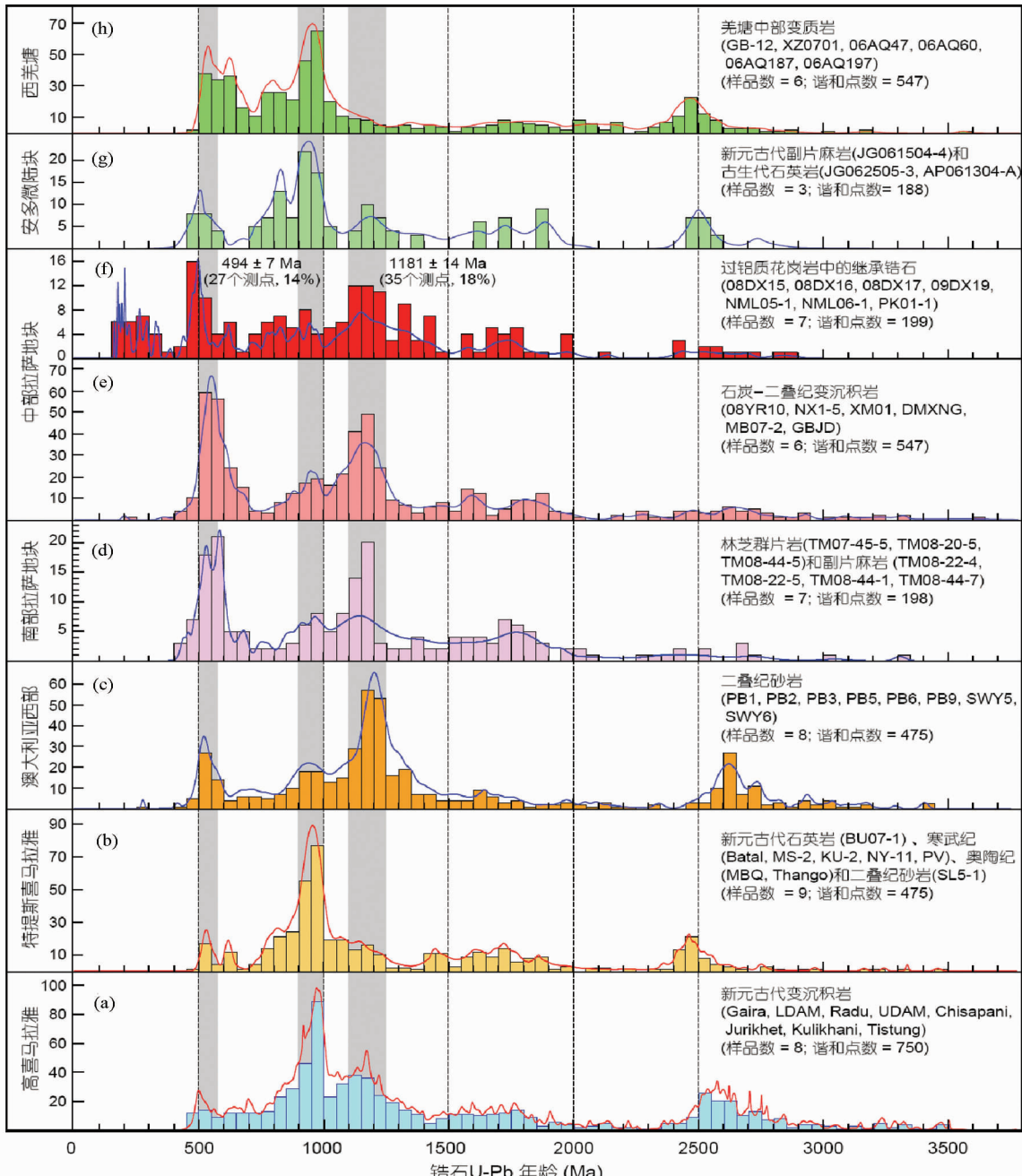


图3 西藏高原碎屑锆石和继承锆石U-Pb年龄频率图(据Zhu et al., 2011a, 2012修改)

图中不考虑谐和度大于10%的测点;对大于1000 Ma的锆石,采用 $^{207}\text{Pb}/^{206}\text{Pb}$ 年龄,对小于1000 Ma的锆石,采用 $^{206}\text{Pb}/^{238}\text{U}$ 年龄。澳大利亚西部碎屑锆石数据(Cawood and Nemchin, 2000; Veevers et al., 2005),其它数据来源同图1

Fig. 3 Age distributions of detrital zircons and inherited zircons from the Tibetan Plateau (modified after Zhu et al., 2011a, 2012)

Zhu et al., 2009a)有关。

5 讨论

5.1 拉萨地块过铝质花岗岩继承锆石年龄特征及其与拉萨地块古生代沉积岩碎屑锆石的对比

本文在当雄宁中、谷露等地3件早侏罗世过铝质花岗岩

样品中获得了95个测点的谐和继承锆石年龄数据,结合近年在工布江达西侧报道的皮康中二叠世(样品PK01-1共25个测点; Zhu et al., 2009a)、南木林罗扎地区晚三叠世(样品NML05-1N、ML06-1共62个测点)和当雄谷露地区早侏罗世(样品08DX17共17个测点)过铝质花岗岩(Zhu et al., 2011b)(图1)的继承锆石年龄数据,共7件样品199个谐和测点定义了1250~1100 Ma(峰值为1181 ± 14 Ma)和550~

450Ma(峰值为 494 ± 7 Ma)2个最突出的年龄群(图3f),分别可比于(1)中部拉萨地块石炭-二叠纪变沉积岩(Zhu et al., 2011a; 图3e)和南部拉萨地块林芝群片岩和副片麻岩(Dong et al., 2010; 图3d)中碎屑锆石定义的年龄峰值(约1170Ma);(2)拉萨地块近期发现的寒武纪火山岩浆活动时代(501Ma, 计文化等, 2009; 492Ma, 作者未刊数据)。拉萨地块约1170Ma的继承锆石和碎屑锆石年龄群,明显不同于以大约960Ma年龄峰值为特征的西羌塘(图3h)、安多(图3g)和特提斯喜马拉雅(图3b)新元古代-古生代变沉积岩的碎屑锆石年龄频谱(Zhu et al., 2011a, 2012)。

5.2 拉萨地块过铝质花岗岩继承锆石和古生代沉积岩碎屑锆石的物源区

通常认为,羌塘、安多、拉萨地块和特提斯喜马拉雅沉积岩中1000~1300Ma的碎屑锆石来源于高喜马拉雅,因为Gehrels et al. (2003)在高喜马拉雅奥陶系-泥盆系砂岩中报道的962个测点的碎屑锆石包含大量1.0~1.3Ga锆石。实际上,Gehrels et al. (2003)报道的碎屑锆石年龄频谱,是以800Ma作为标准来确定究竟是采用 $^{207}\text{Pb}/^{206}\text{Pb}$ 年龄(对老锆石)还是采用 $^{206}\text{Pb}/^{238}\text{U}$ 年龄(对年轻锆石)的,这明显不同于后期文献所采用的1000Ma标准(Leier et al., 2007; McQuarrie et al., 2008; Dong et al., 2010; Hu et al., 2010; Pullen et al., 2008)或1200Ma标准(董春艳等, 2011)。这种不同标准的使用,将带来碎屑锆石年龄频谱的明显变化。例如,若对高喜马拉雅新元古代变沉积岩中大于1000Ma的碎屑锆石采用 $^{207}\text{Pb}/^{206}\text{Pb}$ 年龄,其最突出的碎屑锆石年龄指标被重新标定为0.9~1.0Ga(峰值约960Ma; 图3a),而不是基于大于800Ma采用 $^{207}\text{Pb}/^{206}\text{Pb}$ 年龄所得出的1.0~1.3Ga碎屑锆石年龄指标(Gehrels et al., 2006a, b)。因此,将突出峰值年龄约960Ma的西羌塘、安多和特提斯喜马拉雅新元古代-古生代沉积岩碎屑锆石解释为来源于高喜马拉雅甚至印度和南极洲的Eastern Ghats-Rayner地区是没有争议的(Yoshida and Upreti, 2006; Myrow et al., 2010; Zhu et al., 2012)。这是因为已有年代学数据显示,在东冈瓦纳大陆内部,990~900Ma的花岗岩类仅广泛出露在印度大陆架的Eastern Ghats和南极洲的Rayner等地(Fitzsimons, 2000; Meert, 2003)。

需要重点关注的是拉萨地块过铝质花岗岩和古生代沉积岩中大量存在的1250~1100Ma锆石年龄群(峰值约1170Ma)(图3d-f)的物源区,这是因为这个特殊的年龄群在西羌塘(Kapp et al., 2003; Pullen et al., 2008; Zhu et al., 2011b; 董春艳等, 2011)、安多(Guynn et al., 2011)和特提斯喜马拉雅(McQuarrie et al., 2008; Myrow et al., 2010; Zhu et al., 2011b)新元古代-古生代变沉积岩中缺失或微弱(图3b, g, h),而在后几者中非常突出的约950Ma碎屑锆石年龄峰值,却在拉萨地块非常微弱(图3d-f)。这些差异表明,拉萨地块过铝质花岗岩中的约1170Ma继承锆石和古生

代沉积岩中的同期碎屑锆石的物源区不同于西羌塘、安多和特提斯喜马拉雅。

一种可能性是将中部拉萨地块过铝质花岗岩和广泛分布的石炭-二叠系变沉积岩中大量约1170Ma的锆石解释为来源于高喜马拉雅,因喜马拉雅新元古代变沉积岩中包含有1.00~1.25Ga的碎屑锆石(图3a)(Gehrels et al., 2003, 2006a, b)。但问题在于,大约1170Ma时高喜马拉雅并没有发生广泛的岩浆作用,并且如果拉萨地块大约1170Ma的锆石来源于高喜马拉雅,那么,(1)夹持于拉萨地块和高喜马拉雅之间的特提斯喜马拉雅古生代沉积物也应该含有大量约1170Ma的碎屑锆石;(2)夹持于特提斯喜马拉雅和安多、西羌塘之间的拉萨地块也应该含有大量约950Ma的碎屑锆石,但实际情况却并非如此(图3b)。因此,高喜马拉雅不太可能是拉萨地块过铝质花岗岩继承锆石和古生代沉积岩碎屑锆石的潜在物源区(Zhu et al., 2011b)。现有研究表明,在澳大利亚西部和南西部的Nornalup杂岩、Albany-Fraser造山带和东南极Wilkes造山带发育大量1170Ma左右的岩浆岩,而缺失1000~900Ma的岩石(Clark et al., 2000; Fitzsimons, 2000)。这些地区在二叠纪时为澳大利亚西部的Collie盆地和Perth盆地提供了沉积物,导致来自后两者的二叠纪砂岩显示约1170Ma的碎屑锆石年龄峰值(图3c)(Sircombe et al., 1999; Cawood and Nemchin, 2000)。基于拉萨地块古生代沉积岩碎屑锆石和澳大利亚西部二叠纪砂岩碎屑锆石年龄频谱和1170Ma左右碎屑锆石Hf同位素的强烈相似性,Zhu et al. (2011a)提出拉萨地块非常突出的约1170Ma的碎屑锆石,来源于澳大利亚南西部的Albany-Fraser造山带和东南极的Wilkes等地(图4)。因此,本文认为,拉萨地块过铝质花岗岩中出现的大量约1180Ma的继承锆石,与拉萨地块古生代沉积岩的同期碎屑锆石具有相似的最初物源区,即它们都来自澳大利亚南西部Albany-Fraser造山带和东南极Wilkes等地。

拉萨地块过铝质花岗岩中550~450Ma(峰值为 494 ± 7 Ma)的继承锆石,其浑圆状晶体外形指示其经历了长距离搬运或再循环,其物源区可能来自澳大利亚西部,因为在澳大利亚西部和东南极,广泛出现了同期花岗岩类的侵位(Fitzsimons, 2000; Cawood et al., 2007)。但并不排除部分继承锆石来自拉萨地块本地,因为现今已经在拉萨地块识别出了约501Ma(计文化等, 2009)和约492Ma(作者未刊数据)的岩浆活动记录。

5.3 拉萨地块过铝质花岗岩中继承锆石和古生代沉积岩中碎屑锆石的古地理意义

考虑到拉萨地块古生代沉积岩中碎屑锆石年龄和Hf同位素与澳大利亚西部二叠纪砂岩的强烈相似性,Zhu et al. (2011a)提出至少在新元古代末期到古生代最早期(大约530~510Ma以前),拉萨地块还位于澳大利亚大陆北缘,接受来自澳大利亚南西部Albany-Fraser造山带和东南极

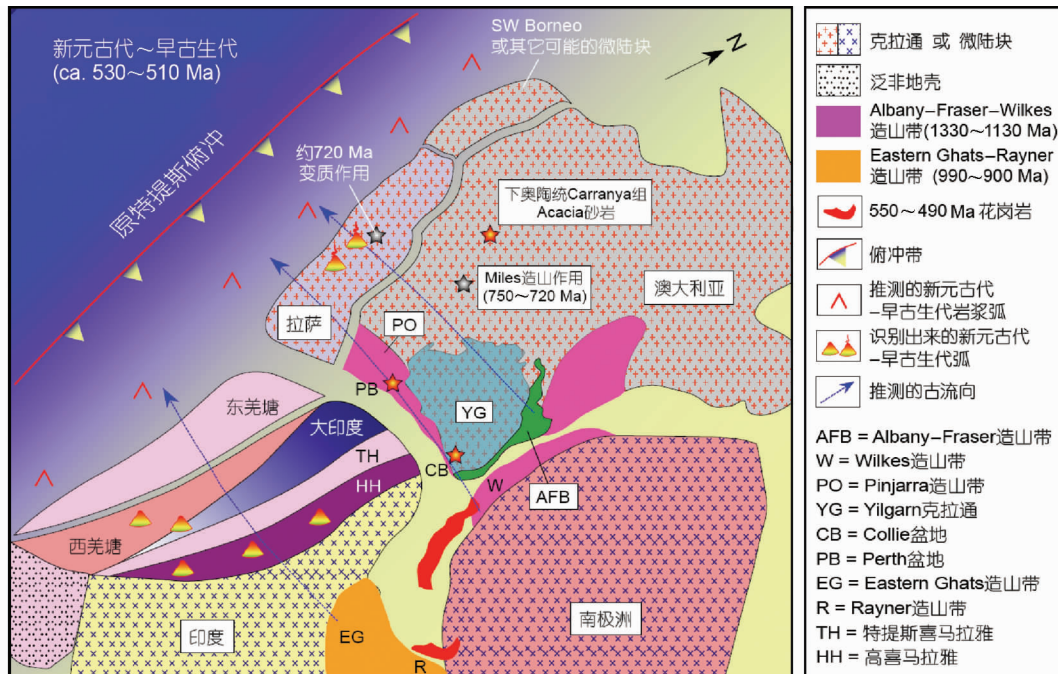


图4 东冈瓦纳 530~510Ma 构造重建图(据 Zhu et al., 2011a 修改)

Fig. 4 Reconstruction of eastern Gondwana at 530 ~ 510Ma (modified after Zhu et al., 2011a)

Wilkes 等地的碎屑沉积(图4),因此拉萨地块与澳大利亚大陆北缘而不是印度大陆北缘具有紧密的古地理联系。本文在拉萨地块过铝质花岗岩中获得的突出的约1180Ma继承锆石群,也支持这一认识。实际上,中部拉萨地块约720Ma的角闪岩相变质年龄(张泽明等,2010)和澳大利亚北部同期发生的Miles造山作用(750~720Ma; Bagas, 2004)(图4)以及突出显示约1170Ma碎屑锆石年龄峰值和明显缺乏约960Ma碎屑锆石记录的澳大利亚北部Canning盆地下奥陶统Carranya组Acacia砂岩(图4)(Haines and Wingate, 2007)等,均指示拉萨地块和澳大利亚北部在新元古代晚期很可能是作为一个整体连在一起的。

在所有古生代时期的冈瓦纳大陆重建模型中,在其北缘都描述了一系列微陆块或地体(即基梅里微陆块,包括土耳其、伊朗、阿富汗、羌塘、拉萨、SW Borneo、保山和Sibumasu等)(Sengör, 1987; Metcalfe, 2009)。虽然一致认为它们均直接或间接来源于冈瓦纳大陆,但不同微陆块或地体所涉及的具体古地理位置仍然未能得到很好约束(Metcalfe, 2009)。拉萨地块的研究实践表明,其可能并非如传统认为的那样裂离自印度大陆北缘,也不是古特提斯南部羌塘→拉萨→大印度→喜马拉雅被动大陆边缘的一部分,而是起源于澳大利亚大陆北缘,作为澳大利亚大陆的一部分经历其新元古代-古生代演化历史(Zhu et al., 2011a, 2012)。因此,拉萨地块过铝质花岗岩继承锆石和古生代沉积岩碎屑锆石的研究实践,可能对进一步约束冈瓦纳大陆北缘其它微陆块的古地理位置和构造岩浆演化历史具有重要启示意义。

6 结论

拉萨地块过铝质花岗岩来源于成熟地壳物质(如变泥质岩)的部分熔融,属强过铝质S型花岗岩。这些花岗岩中的继承锆石显示1250~1100Ma(峰值为 1181 ± 14 Ma)和550~450Ma(峰值为 494 ± 7 Ma)2个最突出的年龄群,分别可比于拉萨地块古生代沉积岩的碎屑锆石年龄峰值(约1170Ma)和寒武纪火山岩的侵位时代。拉萨地块过铝质花岗岩中约1181Ma的继承锆石,可能与拉萨地块古生代沉积岩的同期碎屑锆石具有相似的最初物源区,即它们都来自澳大利亚南西部Albany-Fraser造山带和东南极Wilkes等地,而约494Ma的继承锆石,既可能来自澳大利亚西部,也可能来自拉萨地块本地。本文提供了拉萨地块与澳大利亚大陆具有古地理联系的过铝质花岗岩继承锆石证据,对重建冈瓦纳大陆北缘其它微陆块的古地理具有重要启示意义。

References

- Allègre CJ, Courtillot V, Tapponnier P and other 32 co-authors. 1984. Structure and evolution of the Himalaya-Tibet orogenic belt. *Nature*, 307: 17~22
- Andersen T. 2002. Correction of common lead in U-Pb analyses that do not report ^{204}Pb . *Chemical Geology*, 192: 59~79
- Audley-Charles MG. 1983. Reconstruction of eastern Gondwanaland. *Nature*, 306: 48~50
- Audley-Charles MG. 1984. Cold Gondwana, warm Tethys and the

- Tibetan Lhasa block. *Nature*, 310: 165–166
- Audley-Charles MG. 1988. Evolution of the southern margin of Tethys (North Australian region) from Early Permian to Late Cretaceous. *Geological Society Special Publication*, 37: 79–100
- Bagas L. 2004. Proterozoic evolution and tectonic setting of the northwest Paterson Orogen, Western Australia. *Precambrian Research*, 128: 475–496
- Cawood PA and Nemchin AA. 2000. Provenance record of a rift basin: U/Pb ages of detrital zircons from the Perth Basin, Western Australia. *Sedimentary Geology*, 134: 209–234
- Cawood PA, Johnson MRW and Nemchin AA. 2007. Early Palaeozoic orogenesis along the Indian margin of Gondwana: Tectonic response to Gondwana assembly. *Earth and Planetary Science Letters*, 255: 70–84
- Chung SL, Chu MF, Zhang YQ, Xie YW, Lo CH, Lee TY, Lan CY, Li XH, Zhang Q and Wang YZ. 2005. Tibetan tectonic evolution inferred from spatial and temporal variations in post-collisional magmatism. *Earth-Science Reviews*, 68: 173–196
- Clark DJ, Hensen BJ and Kinny PD. 2000. Geochronological constraints for a two-stage history of the Albany-Fraser Orogen, Western Australia. *Precambrian Research*, 102: 155–183
- Dong CY, Li C, Wan YS, Wang W, Wu YW, Xie HQ and Liu DY. 2011. Detrital zircon age model of Ordovician Wenquan quartzite south of Lungmuco-Shuanghu Suture in the Qiangtang area, Tibet: Constraint on tectonic affinity and source regions. *Science China (Earth Sciences)*, doi: 10.1007/s11430-010-4166-x
- Dong X, Zhang ZM and Santosh M. 2010. Zircon U-Pb chronology of the Nyingtri Group, southern Lhasa Terrane, Tibetan Plateau: Implications for Grenvillian and Pan-African Provenance and Mesozoic-Cenozoic metamorphism. *Journal of Geology*, 118: 677–690
- Dong X, Zhang ZM, Liu F, Wang W, Yu F and Shen K. 2011. Zircon U-Pb geochronology of the Nyainqntanglha Group from the Lhasa terrane: New constraints on the Triassic orogeny of the south Tibet. *Journal of Asian Earth Sciences*, doi: 10.1016/j.jseaes.2011.01.014
- Fitzsimons ICW. 2000. Grenville-age basement provinces in East Antarctica: Evidence for three separate collisional orogens. *Geology*, 28: 879–882
- Gehrels GE, DeCelles PG, Martin A, Ojha TP, Pinhassi G and Upadhyay BN. 2003. Initiation of the Himalayan Orogen as an Early Paleozoic thin-skinned thrust belt. *GSA Today*, 13: 4–9
- Gehrels GE, DeCelles PG, Ojha TP and Upadhyay BN. 2006a. Geologic and U-Th-Pb geochronologic evidence for Early Paleozoic tectonism in the Kathmandu thrust sheet, Central Nepal Himalaya. *Geological Society of America Bulletin*, 118: 185–198
- Gehrels GE, DeCelles PG, Ojha TP and Upadhyay BN. 2006b. Geologic and U-Pb geochronologic evidence for Early Paleozoic tectonism in the Dadeldhura thrust sheet, far-west Nepal Himalaya. *Journal of Asian Earth Sciences*, 28: 385–408
- Guynn JH, Kapp P, Pullen A, Gehrels G, Heizler M and Ding L. 2006. Tibetan basement rocks near Amdo reveal “missing” Mesozoic tectonism along the Bangong suture, Central Tibet. *Geology*, 34: 505–508
- Guynn J, Kapp P, Gehrels G and Ding L. 2011. U-Pb geochronology of basement rocks in central Tibet and paleogeographic implications. *Journal of Asian Earth Sciences*, in revision
- Haines PW and Wingate MTD. 2007. Contrasting depositional histories, detrital zircon provenance and hydrocarbon systems: Did the Larapintine Seaway link the Canning and Amadeus basins during the Ordovician? In: Munson TJ and Ambrose GJ (eds.). *Proceedings of the Central Australian Basins Symposium (CABS)*. Northern Territory Geological Survey, Central Australian Basins Symposium, Alice Springs, Northern Territory, 16–18 August, 2005, Proceedings; Special Publication, no. 2, 36–51
- Hu DG, Wu ZH, Jiang W and Ye PS. 2004. Geochronological studies on the deformation and metamorphism of the Precambrian gabbro from the western area of Nam Co, northern Tibet. *Acta Petrologica Sinica*, 20(3): 627–632 (in Chinese with English abstract)
- Hu XM, Jansa L, Chen L, Griffin WL, O'Reilly SY and Wang JG. 2010. Provenance of Lower Cretaceous Wölong Volcaniclastics in the Tibetan Tethyan Himalaya: Implications for the final breakup of Eastern Gondwana. *Sedimentary Geology*, 223: 193–205
- Ji WH, Chen SJ, Zhao ZM, Li RS, He SP and Wang C. 2009. Discovery of the Cambrian volcanic rocks in the Xainza area, Gangdese orogenic belt, Tibet, China and its significance. *Geological Bulletin of China*, 9: 1350–1354 (in Chinese with English abstract)
- Ji WQ, Wu FY, Chung SL, Li JX and Liu CZ. 2009. Zircon U-Pb chronology and Hf isotopic constraints on the petrogenesis of Gangdese batholiths, southern Tibet. *Chemical Geology*, 262: 229–245
- Kapp JLD, Harrison TM, Kapp P, Grove M, Lovera OM and Ding L. 2005. Nyainqntanglha Shan: A window into the tectonic, thermal, and geochemical evolution of the Lhasa block, southern Tibet. *Journal of Geophysical Research*, 110: B08413, 23
- Kapp P, Murphy MA, Yin A, Harrison TM, Ding L and Guo JR. 2003. Mesozoic and Cenozoic tectonic evolution of the Shiquanhe area of western Tibet. *Tectonics*, 22: 1029, doi: 10.1029/2001TC001332
- Lee HY, Chung SL, Lo CH, Ji J, Lee TY, Qian Q and Zhang Q. 2009. Eocene Neotethyan slab breakoff in southern Tibet inferred from the Linzizong volcanic record. *Tectonophysics*, 477: 20–35
- Leier AL, Kapp P, Gehrels GE and DeCelles PG. 2007. Detrital zircon geochronology of Carboniferous-Cretaceous strata in the Lhasa Terrane, Southern Tibet. *Basin Research*, 19: 361–378
- Li C, Zhai GY, Wang LQ, Yin FG and Mao XC. 2009. An important window for understanding the Qinghai-Tibet Plateau: A review on research progress in recent years of Qiangtang area, Tibet. *Geological Bulletin of China*, 28: 1169–1177 (in Chinese with English abstract)
- Liu QS, Jiang W, Jian P, Ye PS, Wu ZH and Hu DG. 2006. The zircon SHRIMP U-Pb age and petrochemical and geochemical features of Mesozoic muscovite monzonitic granite at Ningzhong, Tibet. *Acta Petrologica Sinica*, 22(3): 643–652 (in Chinese with English abstract)
- Liu Y, Gao S, Hu Z, Gao C, Zong K and Wang D. 2010. Continental and oceanic crust recycling-induced melt-peridotite interactions in the Trans-North China Orogen: U-Pb dating, Hf isotopes and trace elements in zircons of mantle xenoliths. *Journal of Petrology*, 51: 537–571
- Liu Y, Hu ZC, Gao S, Günther D, Xu J, Gao CG and Chen HH. 2008. In situ analysis of major and trace elements of anhydrous minerals by LA-ICP-MS without applying an internal standard. *Chemical Geology*, 257: 34–43
- McQuarrie N, Robinson D, Long S, Tobgay T, Grujic D, Gehrels G and Duce M. 2008. Preliminary stratigraphic and structural architecture of Bhutan: Implications for the along strike architecture of the Himalayan system. *Earth and Planetary Science Letters*, 272: 105–117
- Meert JG. 2003. A synopsis of events related to the assembly of eastern Gondwana. *Tectonophysics*, 362: 1–40
- Metcalfe I. 2009. Late Palaeozoic and Mesozoic tectonic and

- palaeogeographic evolution of SE Asia. *The Geological Society, London, Special Publications*, 315: 7–23
- Miller CF. 1985. Are strongly peraluminous magmas derived from pelitic sedimentary sources? *Journal of Geology*, 93: 673–689
- Mo XX, Dong GC, Zhao ZD, Zhou S, Wang LL, Qiu RZ and Zhang FQ. 2005. Spatial and temporal distribution and characteristics of granitoids in the Gangdese, Tibet and implication for crustal growth and evolution. *Geological Journal of China Universities*, 11(3): 281–290 (in Chinese with English abstract)
- Mo XX, Hou ZQ, Niu YL, Dong GC, Qu XM, Zhao ZD and Yang ZM. 2007. Mantle contributions to crustal thickening during continental collision: Evidence from Cenozoic igneous rocks in southern Tibet. *Lithos*, 96: 225–242
- Mo XX, Niu YL, Dong GC, Zhao ZD, Hou ZQ, Zhou S and Ke S. 2008. Contribution of syncollisional felsic magmatism to continental crust growth: A case study of the Paleocene Linzizong volcanic succession in southern Tibet. *Chemical Geology*, 250: 49–67
- Myrow PM, Hughes NC, Goodge JW, Fanning CM, Williams IS, Pengm SC, Bhargava ON, Parcha SK and Pogue KR. 2010. Extraordinary transport and mixing of sediment across Himalayan central Gondwana during the Cambrian-Ordovician. *Geological Society of America Bulletin*, 122: 1660–1670
- Pan GT, Ding J, Yao DS and Wang LQ. 2004. Guidebook of 1:1500000 Geologic Map of the Qinghai-Xizang (Tibet) Plateau and Adjacent Areas. Chengdu: Cartographic Publishing House, 1–148
- Pan GT, Wang LQ and Zhu DC. 2004. Thoughts on some important scientific problems in regional geological survey of the Qinghai-Tibet Plateau. *Geological Bulletin of China*, 23(1): 12–19 (in Chinese with English abstract)
- Pan GT, Mo XX, Hou ZQ, Zhu DC, Wang LQ, Li GM, Zhao ZD, Geng QR and Liao ZL. 2006. Spatial-temporal framework of the Gangdese Orogenic Belt and its evolution. *Acta Petrologica Sinica*, 22: 521–533 (in Chinese with English abstract)
- Pullen A, Kapp P, Gehrels GE, Vervoort JD and Ding L. 2008. Triassic continental subduction in central Tibet and Mediterranean-style closure of the Paleo-Tethys Ocean. *Geology*, 36: 351–354
- Sengör AMC. 1987. Tectonics of the Tethysides: Orogenic collage development in a collisional setting. *Annual Review of Earth and Planetary Sciences*, 15: 213–244
- Sirccombe KN and Freeman MJ. 1999. Provenance of detrital zircon on the Western Australian coastline: Implications for the geological history of the Perth Basin and denudation of the Yilgarn Craton. *Geology*, 27: 879–882
- Sylvester PJ. 1998. Postcollisional strongly peraluminous granites. *Lithos*, 45: 29–44
- Veevers JJ, Saeed A, Belousova EA and Griffin WL. 2005. U-Pb ages and source composition by Hf-isotope and trace-element analysis of detrital zircons in Permian sandstone and modern sand from southwestern Australia and a review of the paleogeographical and denudational history of the Yilgarn Craton. *Earth-Science Reviews*, 68: 245–279
- Xu RH, Schärer U and Allègre CJ. 1985. Magmatism and metamorphism in the Lhasa block (Tibet): A geochronological study. *Journal of Geology*, 93: 41–57
- Yang JS, Xu ZQ, Li ZL, Xu XZ, Li TF, Ren YF, Li HQ, Chen SY and Robinson PT. 2009. Discovery of an eclogite belt in the Lhasa block, Tibet: A new border for Paleo-Tethys? *Journal of Asian Earth Sciences*, 34: 76–89
- Yin A and Harrison TM. 2000. Geologic evolution of the Himalayan Tibetan Orogen. *Annual Review of Earth and Planetary Sciences*, 28: 211–280
- Yoshida M and Upreti BN. 2006. Neoproterozoic India within East Gondwana: Constraints from recent geochronologic data from Himalaya. *Gondwana Research*, 10: 349–356
- Zhang HF, Harris N, Parrish R, Kelley S, Zhang L, Rogers N, Argles T and King J. 2004. Causes and consequences of protracted melting of the mid-crust exposed in the North Himalayan antiform. *Earth and Planetary Science Letters*, 228: 195–212
- Zhang HF, Xu WC, Guo JQ, Zong KQ, Cai HM and Yuan HL. 2007. Indosinian orogenesis of the Gangdese terrane: Evidences from zircon U-Pb dating and petrogenesis of granitoids. *Earth Science*, 32(2): 155–166 (in Chinese with English abstract)
- Zhang ZM, Zhao GC, Santosh M, Wang JL, Dong X and Shen K. 2010. Late Cretaceous charnockite with adakitic affinities from the Gangdese batholith, southeastern Tibet: Evidence for Neo-Tethyan mid-ocean ridge subduction? *Gondwana Research*, 17: 615–631
- Zhang ZM, Dong X, Geng GS, Wang W, Yu F and Liu F. 2010. Precambrian metamorphism of the northern Lhasa Terrane, south Tibet and its tectonic implications. *Acta Geologica Sinica*, 84(4): 449–456 (in Chinese with English abstract)
- Zhu DC, Pan GT, Mo XX, Wang LQ, Liao ZL, Zhao ZD, Dong GC and Zhou CY. 2006. Late Jurassic-Early Cretaceous geodynamic setting in middle-northern Gangdese: New insights from volcanic rocks. *Acta Petrologica Sinica*, 22: 534–546 (in Chinese with English abstract)
- Zhu DC, Pan GT, Chung SL, Liao ZL, Wang LQ and Li GM. 2008. SHRIMP zircon age and geochemical constraints on the origin of Early Jurassic volcanic rocks from the Yeba Formation, southern Gangdese in south Tibet. *International Geology Review*, 50: 442–471
- Zhu DC, Pan GT, Wang LQ, Mo XX, Zhao ZD, Zhou CY, Liao ZL, Dong GC and Yuan SH. 2008. Tempo-spatial variations of Mesozoic magmatic rocks in the Gangdese belt, Tibet, China, with a discussion of geodynamic setting-related issues. *Geological Bulletin of China*, 27(9): 1535–1550 (in Chinese with English abstract)
- Zhu DC, Mo XX, Niu YL, Zhao ZD, Wang LQ, Pan GT and Wu FY. 2009a. Zircon U-Pb dating and in-situ Hf isotopic analysis of Permian peraluminous granite in the Lhasa terrane, southern Tibet: Implications for Permian collisional orogeny and paleogeography. *Tectonophysics*, 469: 48–60
- Zhu DC, Mo XX, Niu YL, Zhao ZD, Wang LQ, Liu YS and Wu FY. 2009b. Geochemical investigation of Early Cretaceous igneous rocks along an east-west traverse throughout the central Lhasa Terrane, Tibet. *Chemical Geology*, 268: 298–312
- Zhu DC, Mo XX, Zhao ZD, Niu YL, Pan GT, Wang LQ and Liao ZL. 2009. Permian and Early Cretaceous tectonomagmatism in southern Tibet and Tethyan evolution: New perspective. *Earth Science Frontiers*, 16(2): 1–20 (in Chinese with English abstract)
- Zhu DC, Mo XX, Zhao ZD, Niu YL, Wang LQ, Chu QH, Pan GT, Xu JF and Zhou CY. 2010. Presence of Permian extension- and arc-type magmatism in southern Tibet: Paleogeographic implications. *GSA Bulletin*, 122: 979–993
- Zhu DC, Zhao ZD, Niu YL, Dilek Y, Wang LQ and Mo XX. 2011a. Lhasa Terrane in southern Tibet came from Australia. *Geology*, 39: 727–730
- Zhu DC, Zhao ZD, Niu YL, Mo XX, Chung SL, Hou ZQ, Wang LQ and Wu FY. 2011b. The Lhasa Terrane: Record of a microcontinent and its histories of drift and growth. *Earth and Planetary Science Letters*, 301: 241–255
- Zhu DC, Zhao ZD, Niu YL, Dilek Y, Hou ZQ and Mo XX. 2012. Origin and evolution of the Tibetan Plateau. (Submitted to *Gondwana Research*, under review)

附中文参考文献

- 董春艳, 李才, 万渝生, 王伟, 吴彦旺, 颜顽强, 刘敦一. 2011. 西藏羌塘龙木错-双湖缝合带南侧奥陶纪温泉石英岩碎屑锆石年龄分布模式: 构造归属及物源区制约. 中国科学(地球科学), 41(3): 299–308.
- 胡道功, 吴珍汉, 江万, 叶培盛. 2004. 藏北纳木错西缘前寒武纪辉长岩变质变形年代学研究. 岩石学报, 20(3): 627–632.
- 计文化, 陈守建, 赵振明, 李荣社, 何世平, 王超. 2009. 西藏冈底斯构造带申扎一带寒武系火山岩的发现及其地质意义. 地质通报, 28(9): 1350–1354.
- 李才, 翟刚毅, 王立全, 尹福光, 毛晓长. 2009. 认识青藏高原的重要窗口——羌塘地区近年来研究进展评述(代序). 地质通报, 28(9): 1169–1177.
- 刘琦胜, 江万, 简平, 叶培盛, 吴珍汉, 胡道功. 2006. 宁中白云母二长花岗岩 SHRIMP 锆石 U-Pb 年龄及岩石地球化学特征. 岩石学报, 22(3): 643–652.
- 莫宣学, 董国臣, 赵志丹, 周肃, 王亮亮, 邱瑞照, 张风琴. 2005. 西藏冈底斯带花岗岩的时空分布特征及地壳生长演化信息. 高校地质学报, 11(3): 281–290.
- 潘桂棠, 王立全, 朱弟成. 2004. 青藏高原区域地质调查中几个重大科学问题的思考. 地质通报, 23(1): 12–19.
- 潘桂棠, 莫宣学, 侯增谦, 朱弟成, 王立全, 李光明, 赵志丹, 耿全如, 廖忠礼. 2006. 冈底斯造山带的时空结构及演化. 岩石学报, 22(3): 521–533.
- 张宏飞, 徐旺春, 郭建秋, 宗克清, 蔡宏明, 袁洪林. 2007. 冈底斯印支期造山事件: 花岗岩类锆石 U-Pb 年代学和岩石成因证据. 地球科学, 32(2): 155–166.
- 张泽明, 董昕, 耿官升, 王伟, 于飞, 刘峰. 2010. 青藏高原拉萨地体北部的前寒武纪变质作用及构造意义. 地质学报, 84(4): 449–456.
- 朱弟成, 潘桂棠, 莫宣学, 王立全, 廖忠礼, 赵志丹, 董国臣, 周长勇. 2006. 冈底斯中北部晚侏罗世-早白垩世地球动力学环境: 火山岩约束. 岩石学报, 22(3): 534–546.
- 朱弟成, 潘桂棠, 王立全, 莫宣学, 赵志丹, 周长勇, 廖忠礼, 董国臣, 袁四化. 2008. 西藏冈底斯带中生代岩浆岩的时空分布和相关问题的讨论. 地质通报, 27(9): 1535–1550.
- 朱弟成, 莫宣学, 赵志丹, 牛耀龄, 潘桂棠, 王立全, 廖忠礼. 2009. 西藏南部二叠纪和早白垩世构造岩浆作用与特提斯演化: 新观点. 地学前缘, 16(2): 1–20.